Complex Fit Normalized Site Attenuation for Antennas with Complex Radiation Patterns

Zhong Chen, Michael Foegelle
ETS-Lindgren
1301 Arrow Point Drive
Cedar Park, TX 78613
zhong.chen@ets-lindgren.com
michael.foegelle@ets-lindgren.com

Abstract: Complex Fit Normalized Site Attenuation (CFNSA) is proposed as an improvement over the theoretical model in ANSI C63.5. CFNSA accounts for phase center and antenna pattern variations for complex antennas, such as log periodic dipole arrays (LPDA) by solving for the pattern and phase center parameters using S_{21} at multiple heights. A recent study has shown that a simple antenna pattern such as $\cos^n\theta$ is insufficient to represent that of an LPDA above 500 MHz. This paper studies the feasibility of using a higher order analytical function to characterize the complex patterns of a LPDA. It investigates pattern formulations, which result in realistic antenna patterns with small number of unknowns.

Keywords: CFNSA, NSA, complex antennas, antenna calibration, log periodic dipole arrays

Background

The Complex Fit Normalized Site Attenuation (CFNSA) [1] was proposed as an improvement over the theoretical model in ANSI C63.5 [3] by accounting for phase center and antenna pattern variations. The antenna pattern and phase center of a log periodic dipole array (LPDA) were solved by fitting the theoretical phase and/or magnitude response to the measured height dependent S_{21} between the transmitting and receiving antennas. A simple function for the antenna pattern such as $\cos^n\theta$ was shown to be effective only up to 500 MHz [1]. A recent study [2] has shown that at higher frequencies, antenna patterns become complicated. Since $\cos^n\theta$ can only account for certain beamwidth variations, a more sophisticated pattern formulation is needed to represent the side lobes. It is shown in [2] that by using measured patterns instead of a fitted $\cos^n\theta$, antenna factor (AF) variations among different geometries reduced from approximately 1.5 dB to less than 1 dB from 1 to 2 GHz. Note that a perfect model would produce AFs with no variations among calibration geometries (this is the basic characteristic of free-space antenna factors).

As pointed out in [1], a more sophisticated function can be used in the CFNSA method. Because the fitting scheme uses an over determined system of equations, it is possible to have more than one unknown in the pattern formulation. This paper explores the feasibility of using higher order functions (thus more unknowns) for the antenna pattern. Analytical solutions for phased dipole arrays [4] suggest that the antenna pattern is a complex function of cos $b\theta$. It is natural to assume that the LPDA antenna pattern $F(\theta)$ takes on the form:

$$F(\theta) = a_0 + a_1\cos(b\theta) + a_2\cos^2(b\theta) + a_3\cos^3(b\theta) + \ldots + a_N\cos^N(b\theta) \quad (1)$$

where:

$a_0, a_1, \ldots, a_N$ are coefficients for the N^{th} order fit,
b is a normalization constant, and
θ is the observation angle

The higher the order of Equation (1), the more unknowns there are to be solved in the fitting process. It is desirable to have a low order N that can represent a realistic antenna pattern.

LPDA Antenna Patterns

To establish an appropriate function, it is import to understand the patterns of a typical LPDA. Figure 1 to 4 show the measured H-plane patterns of a commercial LPDA with a specified frequency range of 200 MHz to 2 GHz. Zero degree is the boresight direction. Note there is a change in notation from [1], in that 90° is the boresight direction. Either definition yields the same results.

Figure 1 shows the patterns for frequencies from 200 MHz to 500 MHz. It shows that the patterns are relatively simple at these frequencies. A $\cos^n\theta$ function can reasonably represent these patterns. At higher frequencies (Figures 2-4), the patterns get increasingly more complex, and a simple function fails to adequately represent them.

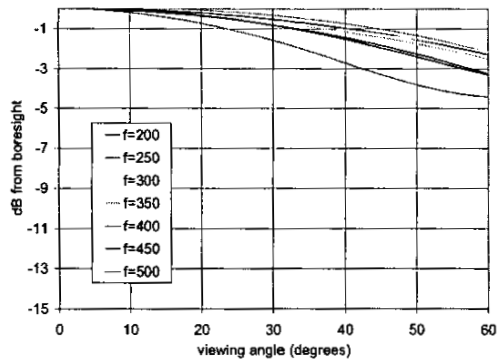

Figure 1. Measured antenna pattern of an LPDA from 200 to 500 MHz (H-plane).

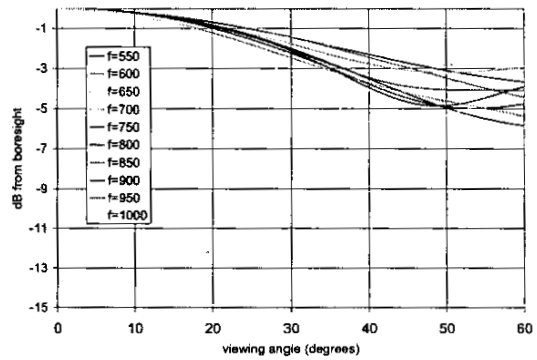

Figure 2. Measured antenna pattern of an LPDA from 550 to 1000 MHz (H-plane).

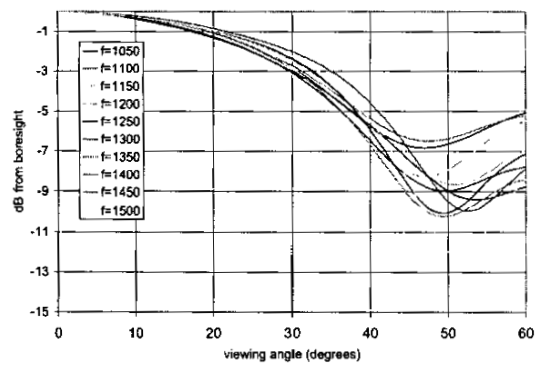

Figure 3. Measured antenna pattern of an LPDA from 1050 to 1500 MHz (H-Plane).

Figure 5 shows the fitted patterns compared to the measured ones at 500 MHz, 1000 MHz, 1500 MHz and 2000 MHz. The fitted patterns use equation (1). Specifically, they use a 4th order fit:

$$F(\theta) = a_0 + a_1\cos(\theta) + a_2\cos^2(\theta) + a_3\cos^3(\theta) + a_4\cos^4(\theta) \quad (2)$$

The graph demonstrates that equation (2) is capable of fitting the patterns for a horizontally polarized antenna (H-plane).

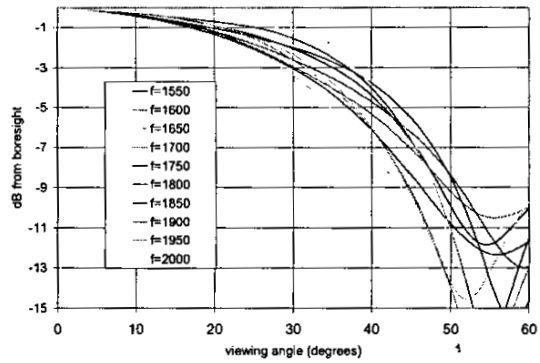

Figure 4. Measured antenna pattern of an LPDA from 1550 MHz to 2000 MHz (H-plane).

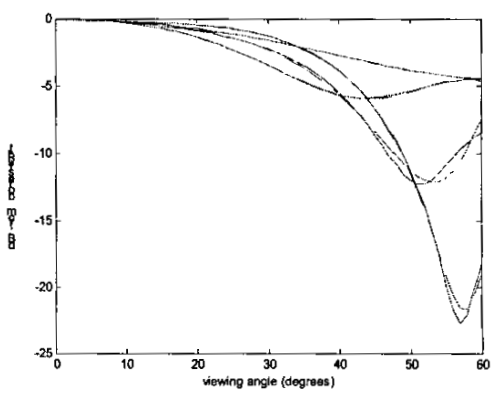

Figure 5. Fitted and measured pattern at 500, 1000, 1500 and 2000 MHz (H-plane). Dashed lines are the fitted, and solid lines are the measured.

Theoretical Background of PCPM

Phase center/Pattern Matching technique was proposed in [1], and is the basis for the fitting scheme here. In summary, for identical antennas with arbitrary pattern, F(θ),

$$E_c = \frac{\sqrt{30P_{rad}D}}{d_1 d_2}\left[d_2 e^{-j\beta d_1}F(\theta_1)^2 + d_1 e^{j(\phi_{h,v}-\beta d_2)}F(\theta_2)^2\left|\rho_{h,v}\right|\right] \quad (3)$$

and

$$CFNSA = \frac{79.58\sqrt{30P_{rad}D}}{2f_M\left|E_C\right|} \quad (4)$$

so that:

$$AF_R = AF_T = \sqrt{SA/CFNSA} \quad (5)$$

where

E_c = electric field generated by a complex antenna in space

P_{rad} = radiated power;

D = directivity of the antenna;

β = wave number in free space;

$\rho_{h,v}$ = reflection coefficient of the ground plane for the horizontal or vertical case;

$\phi_{h,v}$ = reflection coefficient phase angle for the horizontal or vertical case ($\phi_h = \pi$, and $\phi_v = 0$ for perfect electrically conducting ground plane);

d_1 is the distance of the direct ray, given by the formula $d_1 = \sqrt{R^2 + (h_1 - h_2)^2}$;

d_2 is the distance of the reflected ray, given by the formula $d_2 = \sqrt{R^2 + (h_1 + h_2)^2}$;

$\theta_1 = \arccos(\frac{R}{d_1})$

$\theta_2 = \arccos(\frac{R}{d_2})$

R is the separation distance;

h_1 and h_2 are the heights of the transmitting and receiving antennas;

f_M = frequency in MHz

SA is the site attenuation between the two antennas, and

AF_R and AF_T are free space antenna factors of the receive and transmit antennas

For the PCPM fitting, we sum the squares at all possible combinations of heights h_2=b_1, b_2, b_3 ... b_N, and minimize the total residual ξ. In dB form, it becomes

$$\sqrt{\frac{\sum_{i=1}^{N-1}\sum_{j=i+1}^{N}\left|\left(SA(h_2=b_j)-SA(h_2=b_i)\right)-\left(E_C(h_2=b_i)-E_C(h_2=b_j)\right)\right|^2}{N(N+1)/2}}=\xi, \quad (6)$$

where $SA(h)$ is the measured magnitude or phase of site attenuation at height h, and E_c uses either magnitude or phase of Equation (3) accordingly.

With a 4th order fit, there will be 6 unknowns in Equation (6) (a_0 through a_4, plus the separation distance R). The values of $<a_0, a_1, a_2, a_3, a_4, R>$ that minimize the total residual, ξ, in (6) are the desired solution. Conceivably, the a_0 term is not necessary, as it contains no information on the shape of the patterns. The patterns must be properly normalized for θ = 0 in that case. The topic on reducing parameters will be explored in a future study.

An efficient minimum searching algorithm can significantly reduce the solve time. Conventional algorithms, such as a simplex method, suffer from the fact that they can be trapped in local minima. In this paper, a Genetic Algorithm [5] using a float representation is used. Numerical experiments show much improved results by using the genetic algorithm over the conventional hill climbing methods.

Experimental Results

This study uses the same set of experimental data as in [2]. Test data was obtained using a superior quality 50x80 m open area test site having specialized antenna mast and transmit antenna support to provide precise positioning (±0.5 mm) and alignment (±0.5°). Data was acquired for two different makes and models of LPDAs. Antenna A has an operating range of 200-2000 MHz, and antenna B has an operating range of 200-1000 MHz.

Height Dependence

Fundamentally, PCPM scheme fits the shape of E_c as a function of height to that of the measured data. A fit with a small residual indicates the predicted pattern and phase center position can realistically represent the physical behavior between two complex antennas. Figures 6-11 show the variation in the measured, complex fit, and ANSI predicted height dependence of Antenna A at 460, 953.75, and 1493.75 MHz. Notice the improvement in the quality of fit over the original CFNSA with the $\cos^n\theta$ fit at 953.75 MHz (comparing to Figure 2 in [2]).

As frequency goes higher, there is evidence that the quality of fit starts to get worse. At higher frequencies, the antenna boom cross-sectional size is a significant portion of the wavelength. This non-ideal case means that the phase center may actually be off the main axis of the antenna. It is likely that the phase center is not a single point, but rather appears at a variable position as a function of angle from boresight. In addition, cross-polarization due to the staggering design of the dipole elements becomes more important as frequency goes up. Another factor affecting the fit is that even though the Genetic Algorithm is more robust than other fitting methods, it still may not find the global minimum as the general SA response shape gets more complicated at higher frequencies. These effects, as well as methods to improve the algorithms for fitting, will be investigated in a later study.

Antenna Factors

Ideally, antenna factors will have no dependence on calibration or NSA geometry. The spread of AFs under different geometries can therefore be used as an indicator of how well the theory predicts the physically behaviors of the two antennas. Figure 12 and 14 show the ANSI geometry specific antenna factors (GSAF) for antennas A and B, while Figure 13 and 15 show their corresponding complex fit antenna factors (CFAF). There is visible improvement for CFAF except for some glitches, especially for Antenna A at slightly over 1000 MHz for the geometry d=3 m, h_1=2m. This geometry proves to be

challenging for PCPM, because the reflect ray angle can reach approximately 63°.

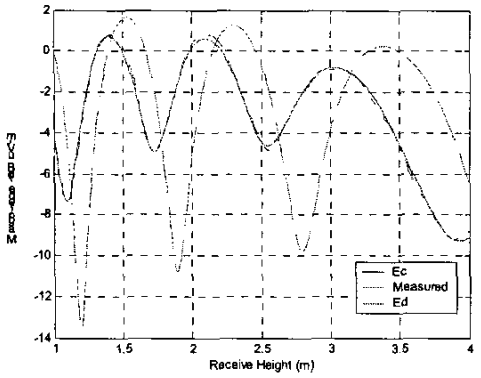

Figure 6. Height dependence of magnitude data comparing CFNSA E_c fit to ANSI E_d and measured data for antenna A, horizontally polarized, 3m separation, 2m transmit height, 470 MHz.

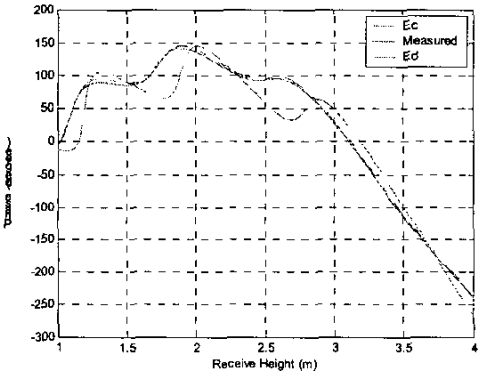

Figure 7. Height dependence of phase data comparing CFNSA E_c fit to ANSI E_d and measured data for antenna A, horizontally polarized, 3m separation, 2m transmit height, 470 MHz.

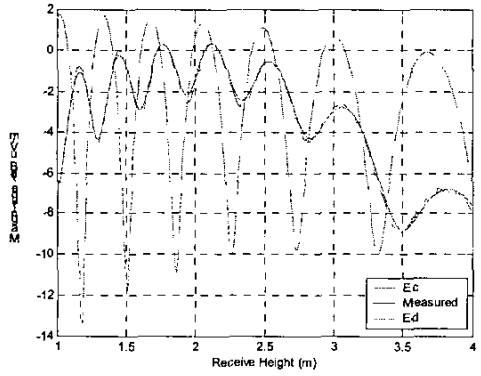

Figure 8. Height dependence of magnitude data comparing CFNSA E_c fit to ANSI E_d and measured data for antenna A, horizontally polarized, 3m separation, 2m transmit height, 953.75 MHz.

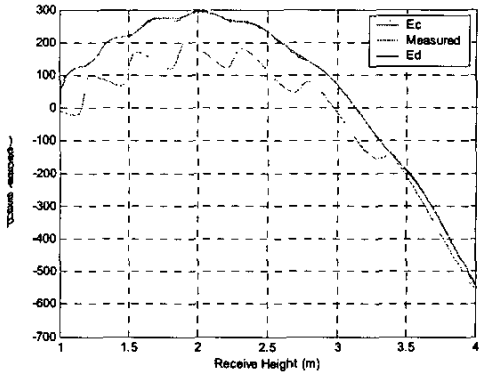

Figure 9. Height dependence of phase data comparing CFNSA E_c fit to ANSI E_d and measured data for antenna A, horizontally polarized, 3m separation, 2m transmit height, 953.75 MHz.

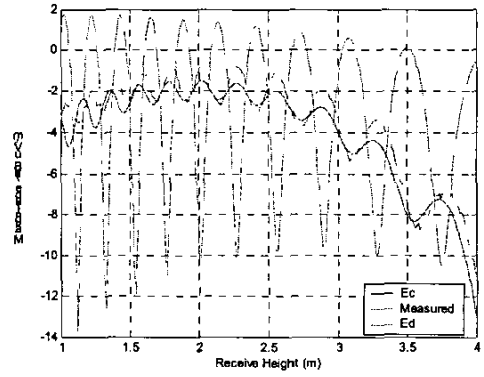

Figure 10. Height dependence of magnitude data comparing CFNSA E_c fit to ANSI E_d and measured data for antenna A, horizontally polarized, 3m separation, 2m transmit height, 1493.75 MHz.

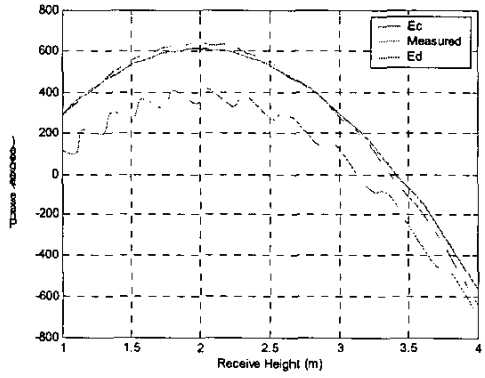

Figure 11. Height dependence of phase data comparing CFNSA E_c fit to ANSI E_d and measured data for antenna A, horizontally polarized, 3m separation, 2m transmit height, 1493.75 MHz.

Besides the improvement ideas mentioned in the previous section, one could also limit the range of height search during the fit, thus limit the pattern angle. For example, at 1493.75MHz (Figure 10), heights above 3 m do not contribute to the final AF (maximum response occurs at approximately 2 m), thus they can be deleted from the fitting analysis. Figures 16 and 17 show the range of variation in the CFAFs vs. that of the GSAFs. Variations within 0.5 dB can be considered identical within the measurement uncertainty. The CFAFs clearly have lower variations at all frequencies but a few glitches.

A phase center vs. frequency graph (Figure 18) can also help detect potential poor fits. The phase center positions predicted by the model show some erratic fluctuations above approximately 1500 MHz for Antenna A. The residuals (Equation (6)) are also direct indicators of the quality of fits.

Higher order antenna pattern functions were experimented with up to 7th order (Equations (1)) for the horizontal antennas above 1000 MHz where the fits are poor. The resulting AFs are not significantly improved. It may be a sign that the pattern magnitude variation is not the dominant effect. At certain frequencies, the peaks and nulls of the magnitude E_c response do not align well with the measured data, which is indicative of other effects mentioned in the earlier section. Primarily, this is likely to be due to phase variation as a function of angle. One possible solution that will be investigated in the future is the use of combined magnitude and phase patterns in place of magnitude only patterns with linear phase center variation.

Vertical polarizations depend on the antenna patterns in the E-plane. Measured antenna patterns [2] have more shape variations in E-plane than in H-plane. Studies by the authors show it is necessary to use a 7th order function or above. Due to time and space limitations, vertical data is not shown in this paper. Results will be presented at the symposium.

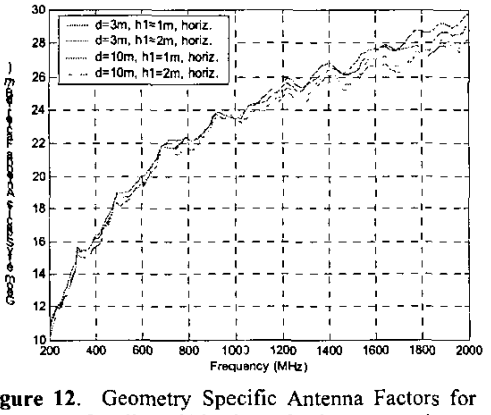

Figure 12. Geometry Specific Antenna Factors for Antenna A for all ANSI horizontal NSA geometries.

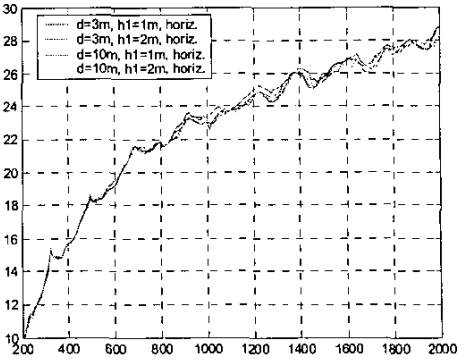

Figure 13. Complex Fit Antenna Factors (dB/m) for Antenna A for all ANSI horizontally polarized NSA geometries.

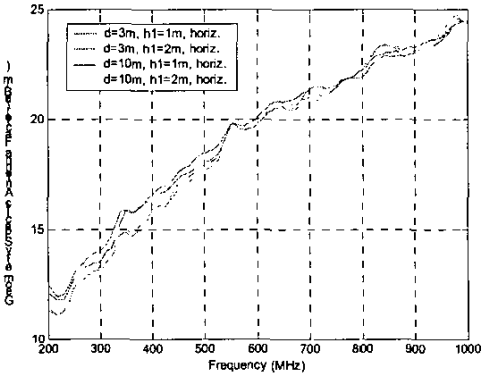

Figure 14. Geometry Specific Antenna Factors (dB/m) for Antenna B for all ANSI horizontally polarized NSA geometries.

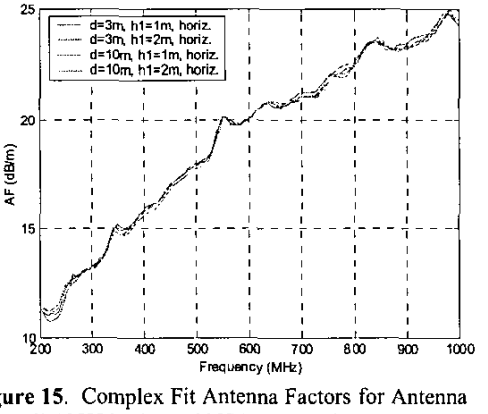

Figure 15. Complex Fit Antenna Factors for Antenna B for all ANSI horizontal NSA geometries.

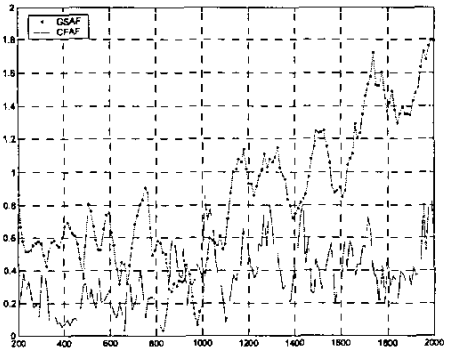

Figure 16. Comparison between the range of variations in dB of CFAFs and GSAFs of Antenna A for all ANSI NSA horizontal geometries.

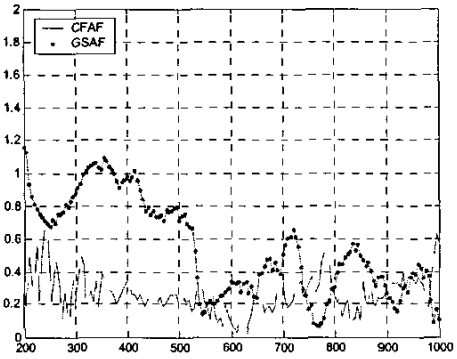

Figure 17. Comparison between the range of variations in dB of CFAFs and GSAFs of Antenna B for all ANSI NSA horizontal geometries.

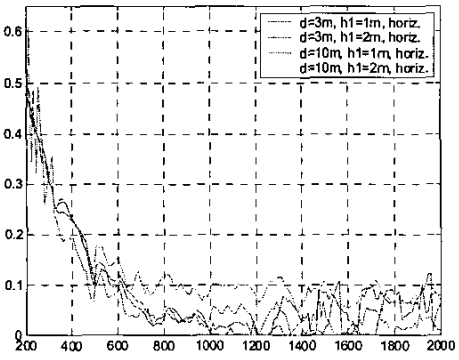

Figure 18. Phase center fits for Antenna A: phase center from the tip of the antenna (m) vs. frequency (MHz).

Conclusions and Summary

It is shown in this paper that it is feasible to use a higher order pattern function to generate CFNSAs. The range of variation in antenna factors is less than 0.9 dB for all horizontal geometries. Improvements can be made in the algorithm to further reduce this variation. By comparison, ANSI GSAFs have a variation of 1.8 dB.

A Genetic Algorithm is proved to be capable of solving the multidimensional problems presented by the CFNSA method. Suggested future studies include the following:

- Further improve the robustness of the fitting algorithm, and better locate the global minima;
- Allow the phase center to vary off-axis, or replace the phase center search with a phase pattern function;
- Limit the height (angle) search;
- Reduce total parameters in the pattern function, or employ other functions such as piecewise functions to represent patterns.

References:

[1] Z. Chen, M. Foegelle, "An Improved Method for Determining Normalized Site Attenuation using Log Periodic Dipole Arrays", *IEEE Intl. Symp. Electromag. Compat.*, Washington, DC, 2000.

[2] M. Foegelle, "An Analysis of the Complex Fit Normalized Site Attenuation Method," *IEEE Intl. Symp. Electromag. Compat.*, Minneapolis, Minnesota, 2002.

[3] ANSI C63.5-1988, *American National Standard For Calibration of Antennas Used for Radiated Emissions Measurements in Electromagnetic Interference (EMI) Control*, American National Standards Institute, New York, 1988.

[4] J. D. Kraus, "Antennas", second edition, Chapter 11, McGraw Hill, 1988.

[5] Houck, Joines, and Kay, "A genetic algorithm for function optimization: a Matlab implementation", *NCSU-IE TR 95-09*, 1995. (http://www.ie.ncsu.edu/mirage/GAToolBox/gaot/)